J Mater Sci: Mater Electron (2020) 31:22162–22170

Effect of filler loading on the shielding of electromagnetic interference of reduced graphene oxide reinforced polypropylene nanocomposites prepared via a twin-screw extruder

Ashish Kaushal[1,*] and Vishal Singh[1]

[1] *Department of Material Science and Engineering, National Institute of Technology, Hamirpur 177005, India*

Received: 28 July 2020
Accepted: 19 October 2020
Published online: 31 October 2020

ABSTRACT

Thermoplastic polypropylene (PP) with different loadings (0.5, 1, 3 & 5 wt%) of reduced graphene oxide (RGO) were prepared to design a nanocomposite to shield the electromagnetic interference (EMI) using melt processing technique via a twin-screw extruder. The nanocomposites were characterized by dc conductivity, mechanical, fractography, and electromagnetic shielding applications. Incorporation of RGO significantly affects the mechanical strength of nanocomposites, which helps to rise in the tensile (4.7%) and flexural strength (4%) at maximum (5 wt%) RGO loading compared to pure PP. There has an improvement in the electrical conductivity of nanocomposites with an increase in the filler load. The RGO/PP nanocomposites exhibit the EMI shielding effectiveness (SE) of − 10.2 dB with 2 mm of thickness at 5 wt% of RGO loading. The outcomes showed that the RGO/PP nanocomposites are able to block up to 90% of the EM wave and are a potential candidate for another kind of microwave absorbing material at large-scale manufacturing division.

1 Introduction

The rapidly growing use of electronic and electrical devices has given a lot of boost to EMI, and there is a need to protect these electronic devices, gadgets from EMI [1]. In general, there are some unwanted emissions from EMI, which cause noise in electronic devices and harmful to the human body [2]. For the arrangement of these issues, it is essential to build up the EMI protecting materials. The underlying mechanisms of EMI include reflection, absorption, and multiple reflections [3]. In the past, metal compounds have been broadly utilized as EMI protecting materials due to their high electrical conductivity and ability to reflect incident electromagnetic waves. Their characteristics, such as heavyweight, low rigidity, and corrosion, limit their use. However, several attempts have been made to develop lightweight coating materials [4, 5]. Polymer compounds containing carbon content are widely used for

Address correspondence to E-mail: ashish.nith14@gmail.com

https://doi.org/10.1007/s10854-020-04719-3

shielding materials over metals due to their advantages such as lightweight, mechanical flexibility, ease of processing, corrosion resistance, adjustable electrical conductivity, and low cost [4, 6, 7]. Conductive polymer compounds are usually prepared for useful materials that protect against electromagnetic interference through conductive fillers such as CNT [8], graphene [9], carbon black [10], and RGO [11] by in situ polymerizations [12] of the monomers, melt mixing [13] or solution mixing [14] of solutions. Graphene-based nanocomposites have received considerable research attention because they have managed to improve the electrical, mechanical as well as shielding properties [15–23].

The reason for selecting RGO as a conductive filler, is its good electrical conductivity, mechanical strength, and higher flexibility. The presence of functional groups and defects creates impedance misalignment and electronic relaxation of dipoles, which generally contributes to increasing electromagnetic interference, especially microwave absorption [24]. Yan et al. [24] studied reduced graphene oxide (RGO)/polystyrene (PS) nanocomposites for EMI shielding applications. The nanocomposites were prepared using solid-phase compression molding and achieved SE of 45.1 dB at 3.47 vol% RGO loading. Kim et al. [25] developed the reduced graphene oxide (RGO) polyetherimide (PEI) films by the electrophoretic deposition technique. They found the prepared PEI/RGO nanocomposites exhibit EMI SE of 6.37 dB at 0.66 vol% of RGO. Sawai et al. [20] studied the EMI SE of RGO filled Polyetherimide (PEI) film nanocomposites for 0.5 to 2.5 weight % of RGO. The measured EMI SE was 22–26 dB in the X-band (8.2–12.4 GHz) frequency range, while the pure PEI indicated the SE of 1–3 dB. Zhu et al. [26] prepared the ferrocobalt magnetic nanoparticle decorated (FeCo)/Reduced graphene oxide (FeCo@rGO)/ Ultrahigh molecular weight polyethylene (UHMWPE) nanocomposites via precipitation method for EMI shielding applications. The FeCo@rGO/UHMWPE nanocomposites showed a good EMI shielding effectiveness of 21.8 dB in the X-band with the presence of 8.97 vol% FeCo@rGO. George et al. [1] studied the polypropylene/reduced graphene oxide (RGO) nanocomposites by latex method using in situ polymerization. That displayed EMI SE of − 50 and − 48 dB in the X- and Ku-band, respectively, at 20 wt % of RGO content.

The melt processing technique is the prominent traditional technique for producing graphene-based polymeric materials as well as suitable for large-scale manufacturing [27–31]. It is important to note that the above studies did not meet the requirement of industrial use and are not suitable for large-scale manufacturing. Although some researchers have used traditional methods to prepare nanocomposites, most of them just focused only on improving the shielding performance and avoided improving the tensile and flexible strength of nanocomposites which are essential for withstanding tension and stress-bearing restorations, when high pressure is exerted on the material.

In this article, the main objective is to prepare the RGO/PP nanocomposite via conventional technique (melt processing) using a twin-screw extruder. This study was carried out, taking into account the effect of RGO material on the electrical, mechanical, and EMI Shielding performance of these nanocomposites.

2 Experimental

2.1 Materials

HMEL, Polysure (India), provided an isotactic homopolymer polypropylene (PP) with a density of 1.8 g/cm^3 and a melt flow index of 12 g/10 min (230 °C/2.16 kg). Reduced graphene oxide (RGO) having a thickness of 2 nm and a diameter of 4 μm purchased from Nanohemzone, India.

2.2 Preparation of RGO/PP nanocomposite

RGO/PP nanocomposite samples were obtained by a twin-screw extruder (Labtech, Thailand 20MM) using a melt processing technique with a mixing time of 10 min, at a processing temperature of 220 °C, and a screw speed of 150 rpm, respectively. The samples were designated as PURE, 0.5 RGO, 1RGO, 3RGO and 5RGO according to 0, 0.5, 1, 3, and 5 wt % of RGO present in it. Samples for the tensile test were made using an injection molding (ARBURG 320 C) machine at a cylinder temperature of 200 °C.

2.3 Characterization

Scanning electron microscopy (SEM) images were scanned using a Quanta FEG450. A two-probe

(Keithley (SCS 2400)) tester was used to measure the electrical conductivity. Tensile properties were evaluated using a universal model of the Zwick-Z010 tester at a speed of 10 mm/min. Three-point bending tests were studied using a universal testing machine (MTEST Quattro). EMI SE was measured over the X-band using an Agilent E8362B vector network analyzer (VNA).

3 Results and discussion

Figure 1a shows the stress–strain relationship of the nanocomposites; it has shown from the Fig. 1a that with the increase in RGO content, the behavior of the nanocomposites changes from ductile to brittle. It is apparent in Fig. 1b that the PRG (RGO reinforced PP) nanocomposites exhibit better tensile strength comparable to the pure PP. The highest value for the tensile modulus achieved at 3 wt% RGO loading is 1022.13 MPa (Fig. 1c). At 0.5 and 1 wt% of RGO loading, the tensile strength is improved than that of pure PP. The decrease in tensile strength has been observed at 3 wt% RGO loading, this is due to the interconnection between RGO and PP which reduced the surface area and subsequently reduced the stress transfer efficiency. However, the tensile strength decreases at 3 wt % RGO loading, which is ascribed to the agglomeration of RGO and reduced stress transmission [32]. However, the tensile strength of the nanocomposite decreases, but it is still higher than the pure polypropylene. This change leads to a decrease in the cross-linkability of the nanocomposites, called mechanical percolation [33].

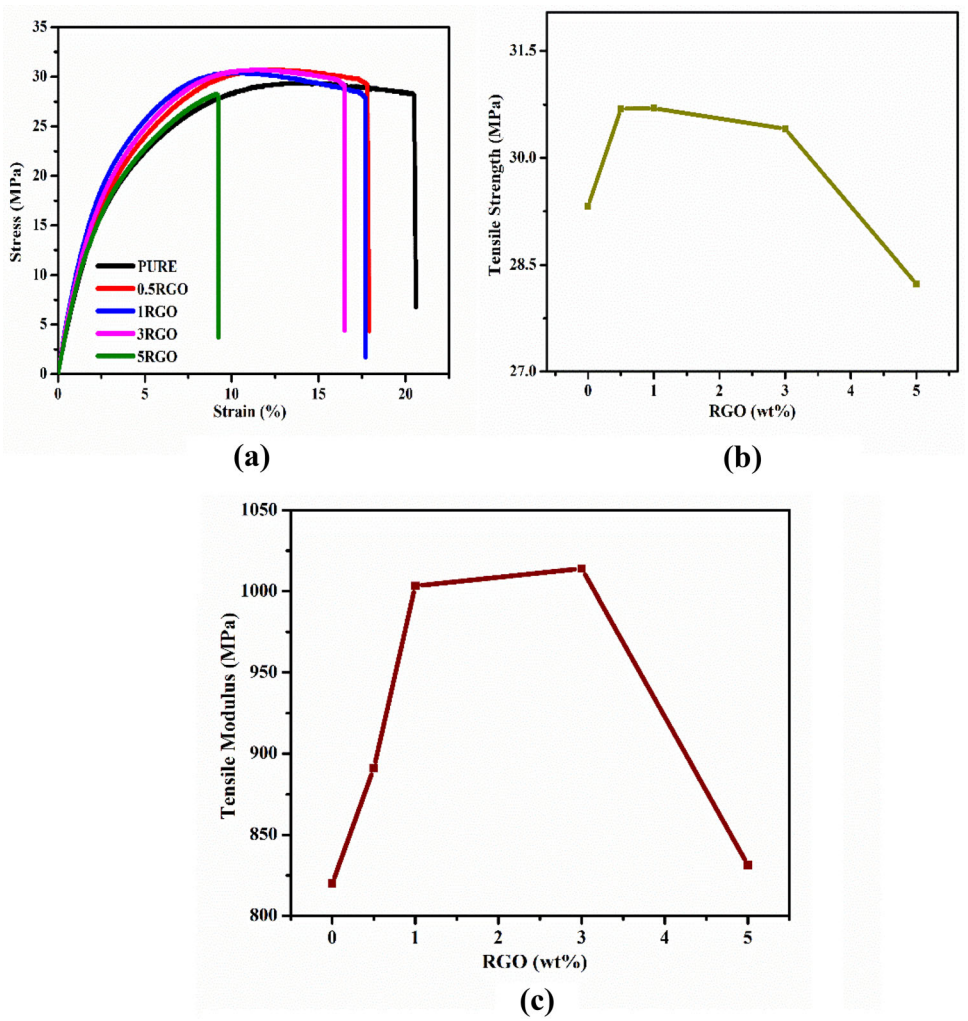

Fig. 1 Results of tensile test: **a** stress–strain curve, **b** tensile strength, **c** and tensile modulus of RGO/PP nanocomposites

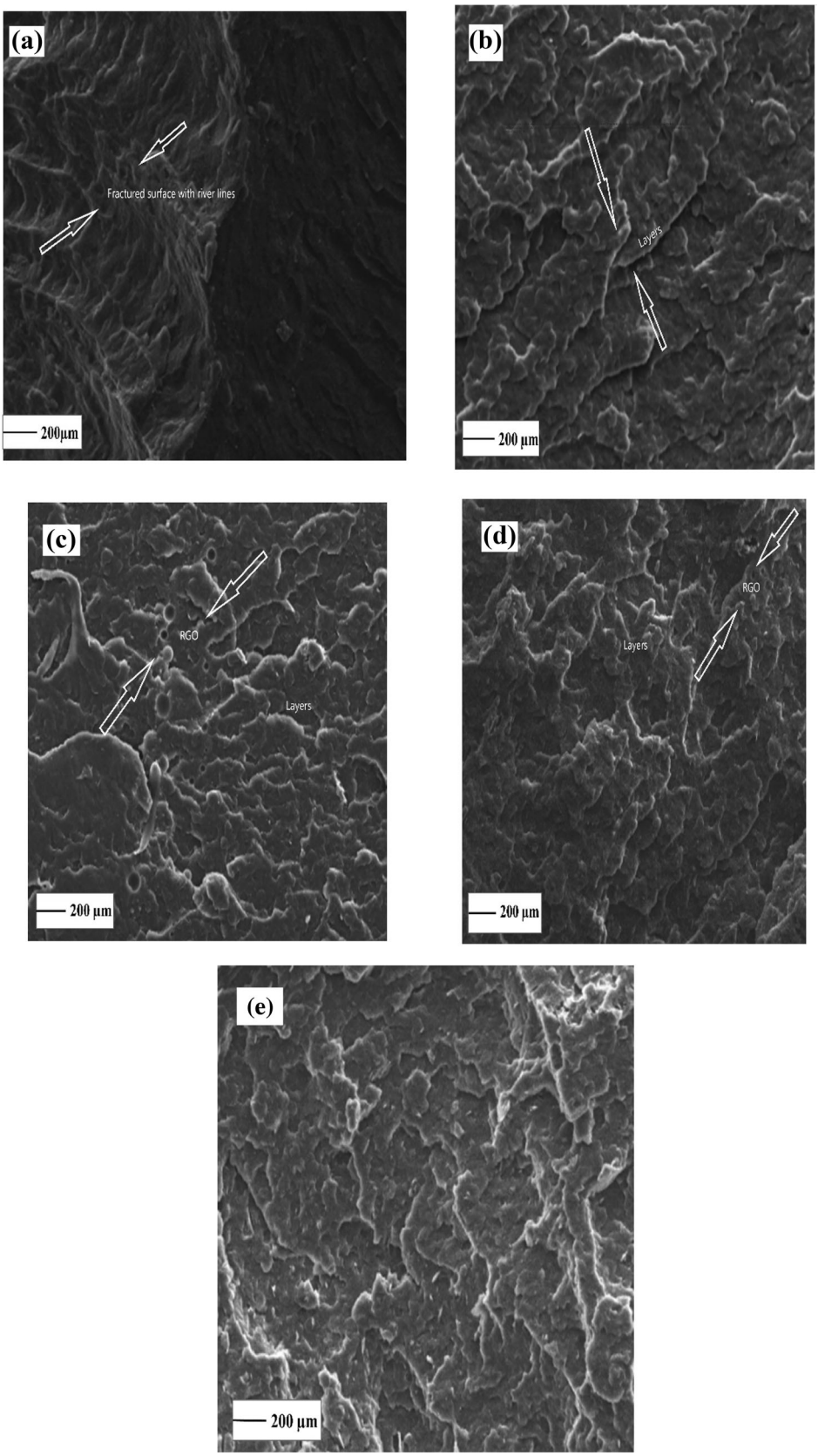

Fig. 2 Fractured SEM images of **a** PURE, **b** 0.5 wt%, **c** 1 wt%, **d** 3 wt%, **e** and 5 wt%, of RGO/PP composites

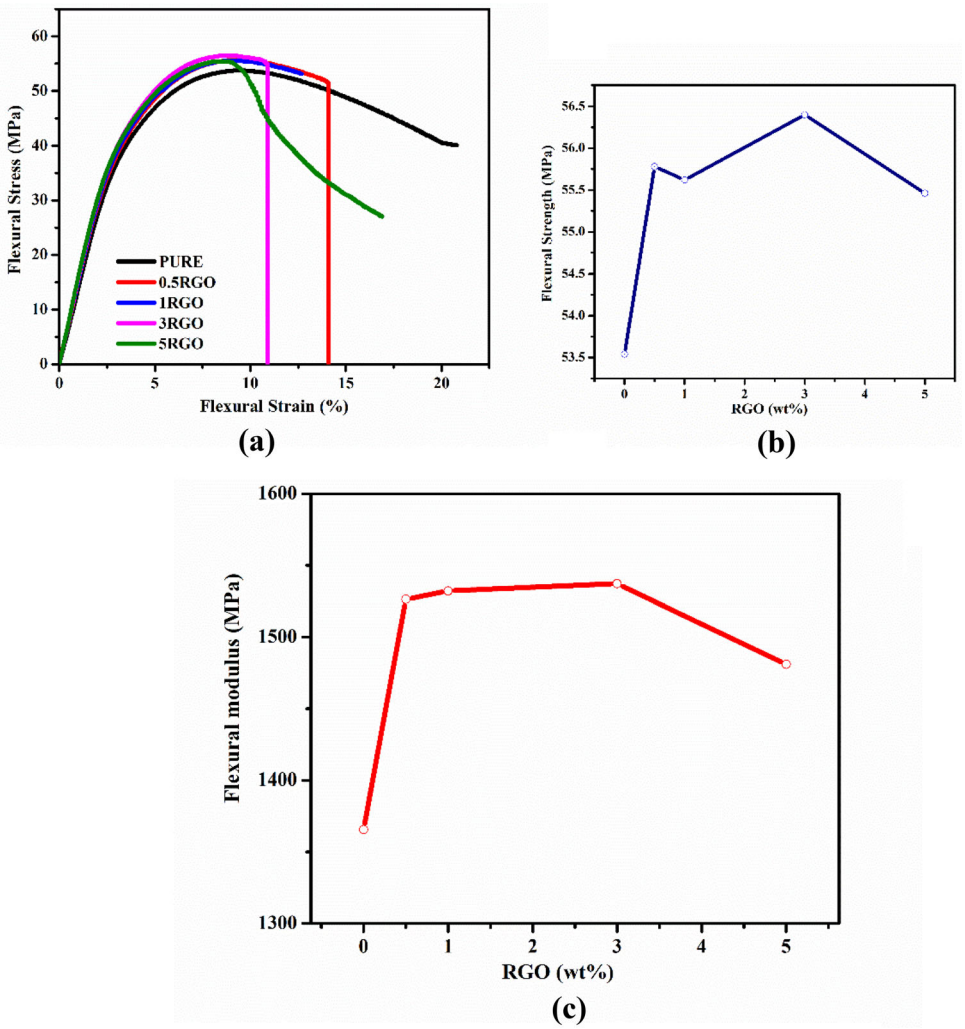

Fig. 3 Results of flexural test: **a** stress–strain curve, **b** flexural strength, **c** and flexural modulus of RGO/PP nanocomposites

3.1 Fracture morphology

Morphologies of the fractured surface of RGO/PP nanocomposites with different weight percent RGO are presented here. The cross-sectional surface of the tensile fracture of pure PP (Fig. 2a) looks like a relatively smooth river line; the lines show that the expansion of PP [34]. The images of RGO/PP nanocomposites showed a rough surface with enlarged edges and areas folded on layered RGO sheets (Fig. 2b) [20]. There are some apparent irregular stretch marks when pulling out the RGO (Fig. 2c). Some irregular stretch marks have been seen, which arise by pulling out of RGO from the nanocomposite (Fig. 2d). The fractured surface is going rougher with the increase in RGO content, and the resulting dislocation increases the tensile modulus of the nanocomposites. (Fig. 2e) [35].

3.2 Flexural properties

The stress–strain results from the varying weight percentage loading of RGO reinforcement on the RGO/PP nanocomposite from the 3-point bend flexural technique are illustrated in Fig. 3a. It has been observed that RGO interfaces have improved the flexible behavior of nanocomposites.

The flexural stress-strain relationship of RGO/PP nanocomposites is depicted in Fig. 3a. It is observed that the nanocomposites with 5 wt% of RGO loading has proved to be the better candidate in terms to provide better flexural strength compared to the rest of the prepared nanocomposite samples. The flexural modulus (Fig. 3c) increases by 12% for 0.5RGO as

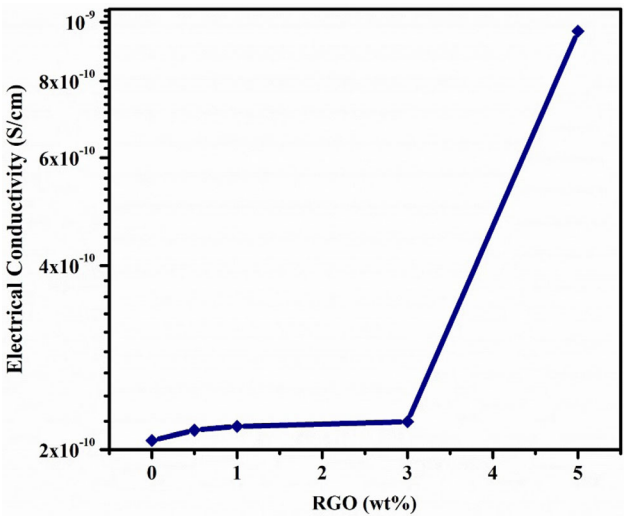

Fig. 4 Electrical conductivity of RGO/PP nanocomposites samples with different weight percentage of RGO

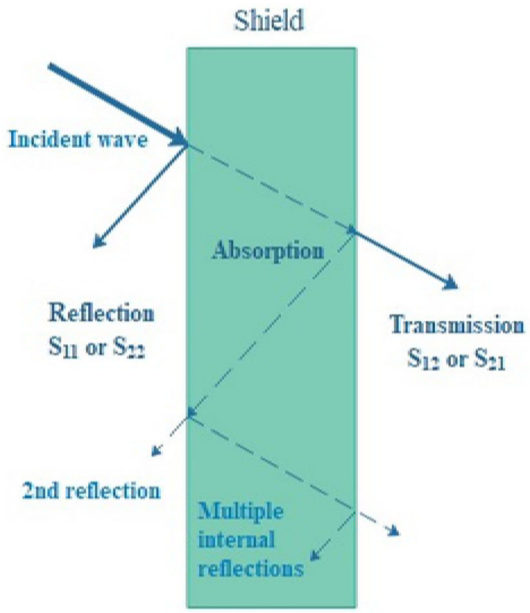

Fig. 5 Schematic of EMI shielding mechanism

compared to pure PP. Increment in modulus is associated with the interphase between the matrix and RGO, which improved the bonding through mechanical adhesion [36]. The flexural strength (Fig. 3b) of RGO containing compounds increases due to better adhesion between RGO and PP. The poor performance of samples with 5 wt % RGO is associated with defects. It has seen at 5 wt% loading of RGO, it agglomerates in the polymer matrix that reduces the strength of the nanocomposite, leading to a decrease in the flexural modulus [37, 38]. RGO as a nanofiller significantly changes the bending strength. These results suggest that the flexural properties of the nanocomposites improved but in a smaller amount.

3.3 Electrical conductivity

The electrical conductivity of the nanocomposites depends on the charge transferred through physical contact between the conductive fillers as well as the conductive network through the insulation gaps between the fillers. A thin layer of insulating polymer forms these gaps, which allows tunneling of electrons from one filler to another through this insulation gap, helps to rise in conductivity [39, 40]. Figure 4 shows an improvement in electrical conductivity at 0.5 and 1 wt % of RGO content. The nanocomposite shows a slight improvement in conductivity at 5 wt% of RGO content, which is 1×10^{-9} S/cm. The rise in conductivity is due to the interconnecting network between the filler and matrix.

3.4 EMI SE

The attenuation is produced by shielding material of the propagating EM waves called EMI shielding. Figure 5 shows the EMI shielding mechanism. EMI can be attenuated by three mechanisms namely absorption, reflection, and multiple reflections. The effect of multiple reflections can be ignored when the absorption loss $\geq$ 10 dB. EMI SE is expressed as the total shielding effectiveness (SE_T) and is described from Eq. (1) which is also the sum of reflection (SE_R), absorption (SE_A), and multi-reflection (SE_M) [41–44].

$$\text{EMI SE}_\text{T} = 10log\frac{P_\text{I}}{P_\text{T}} = 20log\frac{E_\text{I}}{E_\text{T}} = 20log\frac{H_\text{I}}{H_\text{T}}(\text{dB}) \quad (1)$$

where P_I (E_I) and where P_T (E_T) are the power (electric field) of the incident and transmitted EM waves, respectively.

$$\text{SE}_\text{T} = \text{SE}_\text{A} + \text{SE}_\text{R} + \text{SE}_\text{M}(\text{dB}) \quad (2)$$

The results of the measurements of EMI shielding effectiveness over the frequency range of 8.2–12.4 GHz for PP and their composites with various RGO loadings are shown in Fig. 6a–c. In general, there is a vast difference in SE between the pure polymer (PP) and their nanocomposites. Compared to PURE, the EMI SE

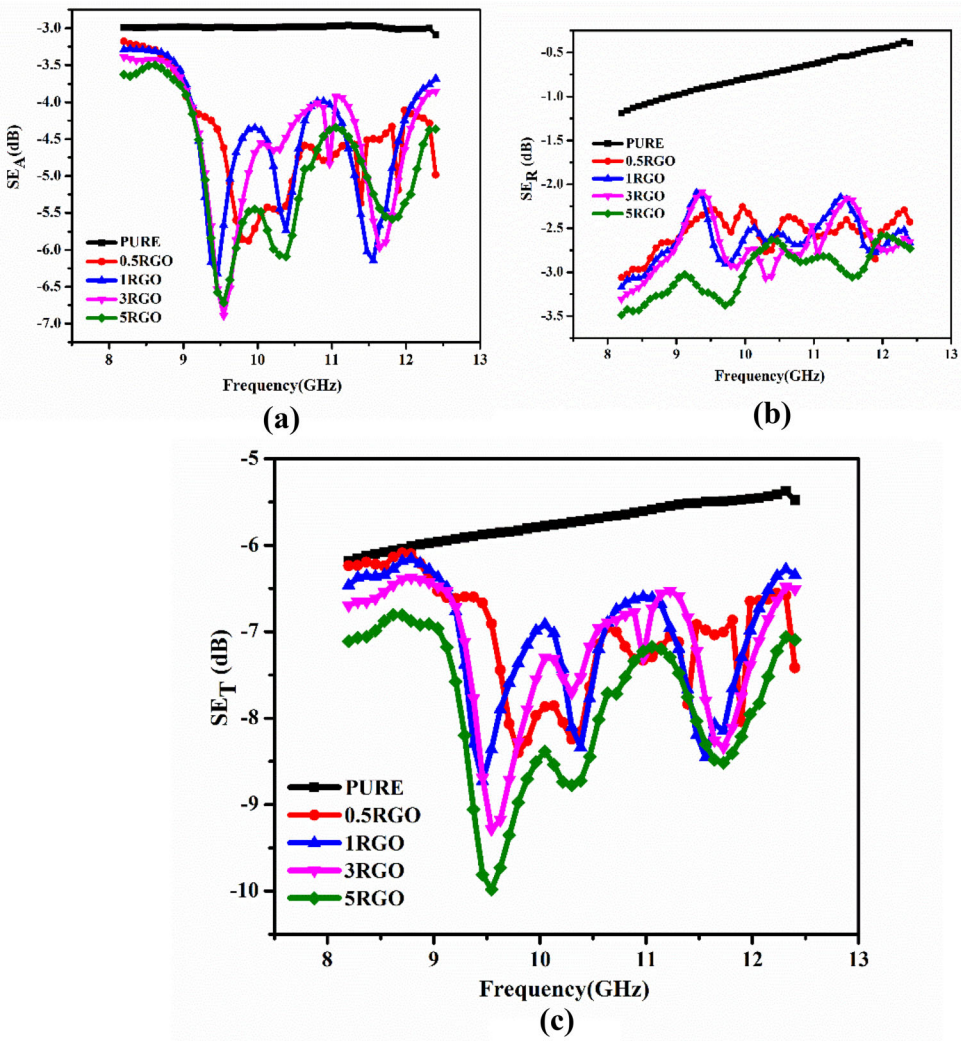

Fig. 6 Diversity of **a** SE_A, **b** SE_R, and **c** SE_T with frequency of RGO/PP nanocomposites

of the nanocomposites increased by 40%. The EMI SE measurement for RGO/PP nanocomposites has done in the X-band frequency range. A rise of 40% in SE is seen at a higher amount of RGO loading as compared to the PURE. As the load increases, the EMI SE of the nanocomposites increases up to − 10.2 dB, respectively, if the coating material can interrupt the 90% of electromagnetic radiation. The rise in EMI SE is mainly associated with the formation of interconnected conductive networks in the polymer matrix [39, 40].

4 Conclusions

RGO reinforced PP nanocomposites were fabricated via melt processing technique using a twin-screw extruder with varying RGO content in the PP matrix. The improvement in mechanical behavior like tensile and flexural strength is increased with the increase in RGO loading. The increase in conductivity has been noticed with the maximum filler loading. EMI shielding properties of the samples were studied in the frequency range of X-band (8.2–12.4 GHz). The EMI SE was measured to be − 10.2 dB with a thickness of 2 mm at 5 wt% of RGO loading. This study provides a valuable polymer nanocomposite with good tensile strength and EMI SE. The prepared nanocomposite is suitable for high-strength EMI shielding materials for on site applications in electronic areas.

References

1. G. George, S.M. Simon, P.V.P. Sajna, M.M. Faisal, R. Wilson, A. Chandran, P.R. Biju, C. Joseph, Green and facile approach

to prepare polypropylene/in situ reduced graphene oxide nanocomposites with excellent electromagnetic interference shielding properties. RSC Adv. **8**, 30412–30428 (2018)
2. M. Blettner, B. Schlehofer, J. Breckenkamp, B. Kowall, S. Schmiedel, U. Reis, P. Potthoff, J. Schu, Mobile phone base stations and adverse health effects: phase 1 of a population-based, cross- sectional study in Germany. Occup. Environ. Med. **66**, 118–123 (2009)
3. M. González, G. Mokry, M. De Nicolás, J. Baselga, J. Pozuelo, Carbon nanotube composites as electromagnetic shielding materials in GHz range. Chem. Rec. **18**, 1–11 (2018)
4. L. Zhang, S. Bi, M. Liu, Lightweight electromagnetic interference shielding materials and their mechanisms, in *Electromagnetic materials*. (IntechOpen, London, 2018). https://doi.org/10.5772/intechopen.82270
5. Y. Bhattacharjee, S. Biswas, S. Bose, *Thermoplastic Polymer Composites for EMI Shielding Applications* (Elsevier Inc, Amsterdam, 2020) https://doi.org/10.1016/B978-0-12-817590-3.00005-1
6. Z. Shen, J. Feng, Preparation of thermally conductive polymer composites with good electromagnetic interference shielding efficiency based on natural wood-derived carbon scaffolds, ACS sustain. Chem. Eng. **7**, 6259–6266 (2019)
7. Z. Chen, C. Xu, C. Ma, W. Ren, H.M. Cheng, Lightweightand flexible graphene foam composites for high-performance electromagnetic interference shielding. Adv. Mater. **25**, 1296–1300 (2013)
8. A.S. Hoang, Electrical conductivity and electromagnetic interference shielding characteristics of multiwalled carbon nanotube filled polyurethane composite films. Adv. Nat. Sci. (2011). https://doi.org/10.1088/2043-6262/2/2/025007
9. J. Ha, S. Hong, J. Ryu, J. Bae, S. Park, Development of multifunctional graphene polymer composites having electromagnetic interference. Polymers **11**(12), 2101 (2019)
10. X. Wang, Investigation of electromagnetic shielding effectiveness of nanostructural carbon black/ABS composites. J. Electromagn. Anal. Appl. **3**, 160–164 (2011)
11. S. Chhetri, P. Samanta, N.C. Murmu, S. Kumar, Electromagnetic interference shielding and thermal properties of non- covalently functionalized reduced graphene oxide/epoxy composites. AIMS Mater. Sci. **4**(1), 61–74 (2016)
12. K. Cheng, H. Li, M. Zhu, H. Qiu, J. Yang, In situ polymerization of graphene-polyaniline@polyimide composite films with high EMI shielding and electrical properties. RSC Adv. **10**, 2368–2377 (2020)
13. N.A. Bhagat, N.K. Shrivastava, S. Suin, S. Maiti, B.B. Khatua, Development of electrical conductivity in PP/HDPE/MWCNT nanocomposite by melt mixing at very low loading of MWCNT. Polym. Compos. **34**, 787–798 (2013)
14. S. Ganguly, P. Bhawal, R. Ravindren, N.C. Das, Polymer nanocomposites for electromagnetic interference shielding: a review. J. Nanosci. Nanotechnol. **18**, 7641–7669 (2018)
15. S. Khasim, Results in physics polyaniline-graphene nanoplatelet composite films with improved conductivity for high performance X-band microwave shielding applications. Results Phys. **12**, 1073–1081 (2019)
16. J. Yan, Y. Huang, C. Wei, N. Zhang, P. Liu, Covalently bonded polyaniline/graphene composites as high- performance electromagnetic (EM) wave absorption materials. Composites A **99**, 121–128 (2017)
17. X. Chen, J. Chen, F. Meng, L. Shan, M. Jiang, X. Xu, J. Lu, Y. Wang, Z. Zhou, Hierarchical composites of polypyrrole/graphene oxide synthesized by in situ intercalation polymerization for high efficiency and broadband responses of electromagnetic absorption. Compos. Sci. Technol. **127**, 71–78 (2016)
18. Y. Wang, X. Gao, Y. Fu, X. Wu, Q. Wang, W. Zhang, C. Luo, Enhanced microwave absorption performances of polyaniline/graphene aerogel by covalent bonding. Composites B **169**, 221–228 (2019)
19. J. Luo, Y. Xu, W. Yao, C. Jiang, J. Xu, Synthesis and microwave absorption properties of reduced graphene oxide-magnetic porous nanospheres-polyaniline composites. Compos. Sci. Technol. **117**, 315–321 (2015)
20. P. Sawai, P.P. Chattopadhaya, S. Banerjee, Synthesized reduce graphene oxide (rGO) filled polyetherimide based nanocomposites for EMI shielding applications. Mater. Today Proc. **5**, 9989–9999 (2018)
21. D.X. Yan, P.G. Ren, H. Pang, Q. Fu, M.B. Yang, Z.M. Li, Efficient electromagnetic interference shielding of lightweight graphene/polystyrene composite. J. Mater. Chem. **22**(36), 18772–18774 (2012)
22. L. Ma, Z. Lu, J. Tan, J. Liu, N. Black, T. Li, J.C. Gallop, L. Hao, Transparent conducting graphene hybrid films to improve electromagnetic interference (EMI) shielding performance of graphene. ACS Appl. Mater. Interfaces **9**, 34221–34229 (2017)
23. M.D. Teli, S.P. Valia, Graphene, C.N.T. based EMI shielding materials introduction to graphene and carbon nanotubes brief outline of synthesis of EMI shielding materials, in *Advanced materials for electromagnetic shielding: fundamentals, properties, and applications*. (Wiley, Hoboken, 2019), pp. 241–261
24. D. Yan, H. Pang, B. Li, R. Vajtai, L. Xu, P. Ren, Structured reduced graphene oxide/polymer composites for ultra-efficient electromagnetic interference shielding. Adv. Funct. Mater. **25**, 559 (2015)
25. S. Kim, J. Oh, M. Kim, W. Jang, M. Wang, Y. Kim, H.W. Seo, Y.C. Kim, J. Lee, Y. Lee, J. Nam, Electromagnetic

interference (EMI) transparent shielding of reduced graphene oxide (RGO) interleaved structure fabricated by electrophoretic deposition. ACS Appl. Mater. Interfaces **6**, 17647–17653 (2014)
26. Y. Zhu, H. Yang, G. Duan, Y. Zhao, Liu, Electromagneticinterference shielding polymer composites with magnetic andconductive FeCo/reduced graphene oxide 3D networks. J. Mater. Sci.: Mater. Electron. **30**, 2045–2056 (2019)
27. D.F. Wu, Y.R. Sun, L. Wu, M. Zhang, Kinetic study on the melt compounding of polypropylene/multi-walled carbon nanotube composites. J. Polym. Sci. B **47**, 608–618 (2009)
28. I. Kim, Y.G.Y.U. Jeong, Polylactide/exfoliated graphite nanocomposites with enhanced thermal stability, mechanical modulus, and electrical conductivity. J. Polym. Sci. B **48**, 850 (2010)
29. H. Zhang, W. Zheng, Q. Yan, Y. Yang, J. Wang, Z. Lu, G. Ji, Z. Yu, Electrically conductive polyethylene terephthalate/graphene nanocomposites prepared by melt compounding. Polymer **51**, 1191–1196 (2010). https://doi.org/10.1016/j.polymer.2010.01.027
30. K. Kalaitzidou, H. Fukushima, L.T. Drzal, Multifunctional polypropylene composites produced by incorporation of exfoliated graphite nanoplatelets. Carbon **45**, 1446–1452 (2007)
31. W. Zheng, X. Lu, S. Wong, Electrical and mechanical properties of expanded graphite-reinforced high-density polyethylene. J. Appl. Polym. Sci. **91**, 2781–2788 (2004)
32. J. Liu, X. Lu, C. Wu, Effect of preparation methods on crystallization behavior and tensile strength of poly (vinylidene fluoride) membranes. Membranes **3**, 389–405 (2013)
33. V. Sriram, G. Radhakrishnan, Novel short-chain crosslinked cationomeric polyurethanes. Polym. Bull. **55**, 165–172 (2005)
34. G.B. Olowojoba, S. Eslava, E.S. Gutierrez, In situ thermally reduced graphene oxide/epoxy composites: thermal and mechanical properties. Appl. Nanosci. **6**, 1015–1022 (2016)
35. L. Zhang, J. Wang, H. Wang, Y. Xu, Z. Wang, Z. Li, Y. Mi, S. Yang, Preparation, mechanical and thermal properties of functionalized graphene/polyimide nanocomposites. Composites A **43**(9), 1537–1545 (2012)
36. H. Mahmood, M. Tripathi, N. Pugno, A. Pegoretti, Enhancement of interfacial adhesion in glass fiber/epoxy composites by electrophoretic deposition of graphene oxide on glass fibers. Compos. Sci. Technol. **126**, 149–157 (2016)
37. C. Zeng, S. Lu, X. Xiao, J. Gao, L. Pan, Ehnaced thermal and mechanical properties of epoxy composites by mixing noncovalently functionalized graphene sheets. Polym. Bull. **72**, 453–472 (2015)
38. J. Gu, Q. Zhang, J. Dang, J. Zhang, S. Chen, Preparation and mechanical properties researches of silane-coupling reagent modified b-silicon carbide filled epoxy composites. Polym. Bull. **62**(5), 689–697 (2009)
39. R. Bera, S. Maiti, B.B. Khatua, High electromagnetic interference shielding with high electrical conductivity through selective dispersion of multiwall carbon nanotube in poly (e - caprolactone)/MWCNT composites. J. Appl. Polym. Sci. **42161**, 1–10 (2015)
40. N. Ryvkina, I. Tchmutin, The deformation behavior of conductivity in composites where charge carrier transport is by tunneling: theoretical modeling and experimental results. Synth. Met. **148**, 141–146 (2005)
41. S. Maiti, N.K. Shrivastava, S. Suin, B.B. Khatua, Polystyrene/MWCNT/graphite nanoplate nanocomposites: efficient electromagnetic interference shielding material through graphite nanoplate– MWCNT–graphite nanoplate networking. ACS Appl. Mater. Interfaces **5**, 4712–4724 (2013)
42. J. Joo, C.Y. Lee, High frequency electromagnetic interference shielding response of mixtures and multilayer films based on conducting polymers High frequency electromagnetic interference shielding response of mixtures and multilayer films based on conducting polymers. J. Appl. Phys. **88**, 513 (2000)
43. A. Ohlan, K. Singh, A. Chandra, V.N. Singh, S.K. Dhawan, Conjugated polymer nanocomposites: synthesis, dielectric, and microwave absorption studies. J. Appl. Phys. **106**, 044305 (2009)
44. Y. Wang, X. Jing, Intrinsically conducting polymers for electromagnetic interference shielding. Polym. Adv. Technol **16**, 344–351 (2005)